(213

IAEA
International Atomic Energy Agency

INDC(NDS)-0530
Distr. SC

INDC International Nuclear Data Committee

Joint ICTP-IAEA Advanced Workshop on Model Codes for Spallation Reactions

International Centre for Theoretical Physics

Trieste, Italy

4 – 8 February 2008

Prepared by

D. Filges[1], S. Leray[2], Y. Yariv[3], A. Mengoni[4], A. Stanculescu[4], G. Mank[4]

[1]Forschungszentrum Jülich GmbH, Germany
[2]CEA-CEN Saclay, France
[3]Soreq Nuclear Research Centre, Israel
[4]International Atomic Energy Agency, Vienna, Austria

August 2008

INCL4 – The Liège INC Model for High-Energy Hadron-Nucleus Reactions

A short description of the INCL4.2 and INCL4.4 versions

A. BOUDARD[1], J. CUGNON[2]

[1] CEA Saclay,
IRFU/SPhN,
Gif-sur-Yvette, France
[2] Department AGO,
University of Liege,
Liege, Belgium

Abstract. The details of the standard INCL4.2 version of the Liège Intranuclear Cascade model for spallation reactions are reviewed. Emphasis is put on the physics features which are incorporated and on their practical implementation in the numerical code. New developments, bearing on the production of clusters, on the properties of the nucleon and pion mean fields and on the behaviour of the model at low incident energy, are briefly presented and discussed. They will be part of the forthcoming INCL4.4 version.

1. Introduction

This report is a short explanatory account of the latest versions of the Liège intranuclear cascade model (INCL) for high-energy nuclear collisions induced by nucleons, pions or light clusters.

The Liège Intranuclear Cascade (INC) model has been built about twenty years ago in order to describe heavy-ion collisions in the GeV range [1]. Afterwards, specific versions have been built to describe reactions induced by antiprotons, pions, nucleons or light clusters. Due to the renewed interest for spallation reactions, in relation to transmutation studies, the early version for nucleon-induced reactions [2] has been improved to give birth to the INCL3 version a few years ago [3] and to the INCL4 version a little bit later [4]. Thanks to the HINDAS collaboration [5], this model was shown to be, when coupled to the ABLA evaporation-fission code, quite successful in describing an extensive set of experimental data in the 200 MeV to 2 GeV energy range [6]. This model, known as INCL4.2, has been included in LAHET [7] and MNCPX [8], and is considered as the standard version of the INCL4 model. It is basically a parameter free model. Yet it suffers from some limited but systematic deficiencies. Further improvements have been studied in the meantime. They bear on the introduction of light charged cluster emission in the cascade stage [9], on the introduction of energy-dependent potentials for nucleons [10], on the introduction of an average potential for pions[11] and on the improvements of the code at low incident energy (below 200 MeV) [12-14]. The inclusion of these developments to the INCL model constitute the version INCL4.4, which is not yet available to the public, some aspects being still under study in the frame of the EUROTRANS collaboration [14]. A version consisting of INCL4.2 plus the production of clusters, as defined in Ref. [9], is available under the label INCL4.3.

The purpose of this note is to describe the standard version of INCL4.2 and to give a short account of the additional features contained in INCL4.4. However, due to lack of space, only the main features of INCL4.2 will be given. For a comprehensive description, we refer to Ref. [15].

2. Description of the standard INCL model (INCL4.2)

2.1. Introduction

The basic premises of the INCL model are schematically illustrated in Fig. 1. Particles are moving freely between instantaneous events that we call "avatars" (to distinguish from the usual meaning of "event", namely a complete simulation or "realization" of the reaction). These avatars can be of three types: two-body collision, decay and transmission or reflection at the nuclear periphery. In INCL4.2 only three types of particles are considered: nucleons *(n, p)*, Δ-isobars (4 charge states) and pions (3 charge states). The target is composed of point-like particles. All particles are followed in space-time and are propagated in single steps between avatars, on a manner described below. The simulation is stopped according to a self-consistent criterion, which constitutes a unique feature of INCL. The properties of the exit channel are recorded and are transferred to an evaporation module.

In this presentation, we will refer to the nucleon-nucleus case, indicating when necessary the variants for incident pions or incident light clusters.

2.2. Description of the model

A. *Target preparation*

Nucleons are positioned at random, according to a distribution *f(r)* which follows nuclear density (i.e. with the same shape), taken from electron scattering measurements. For target mass $A>27$ a Woods-Saxon distribution is used up to a maximum distance R_{max}, fixed to $R_0 + 8a$. For $6<A<27$, a "modified harmonic oscillator" distribution is adopted and for $A<6$, Gaussian density distributions are used. See Ref. [15] for the values of the parameters of these distributions.

Nucleon momenta are taken at random in a sphere of radius pF, the Fermi momentum, equal to 270 MeV/c, a value corresponding to normal nuclear matter. The same distribution is used for protons and neutrons.

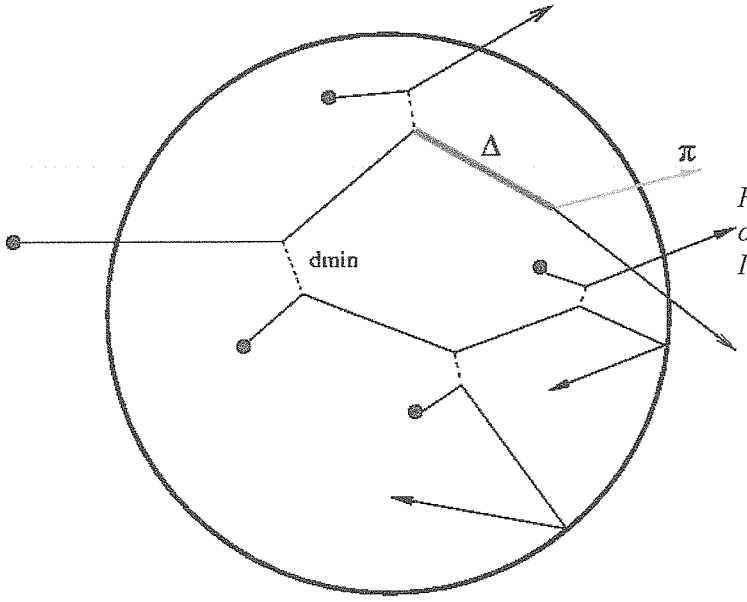

Fig. 1. Schematic illustration of the main features of the INCL model.

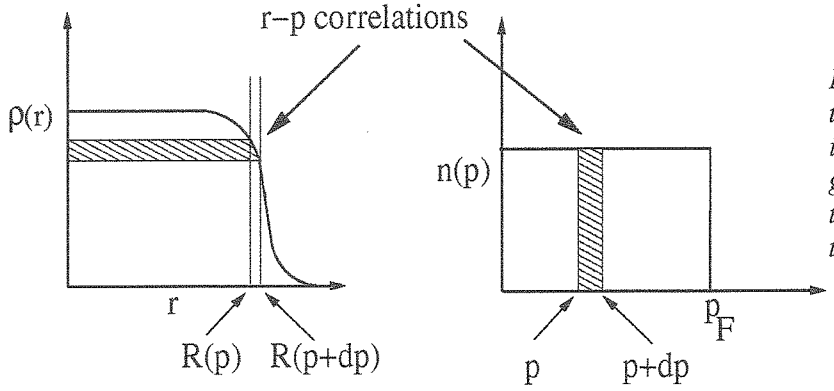

Fig. 2. Illustration of the r-p correlations introduced in the generation of the target initial state. See text for detail.

Actually, momentum and position are not taken independently. Momentum p is generated first at random and the position is taken at random inside a sphere of radius $R(p)$, which is implicitly given by:

$$\left(\frac{p}{p_F}\right)^3 = -\frac{1}{3N}\int_0^{R(p)} \frac{df(r)}{dr} r^3 dr \tag{1}$$

where N is a normalization constant

$$N = \int_0^{R_{max}} f(r) r^2 dr \tag{2}$$

It is easy to check that $R(p)$ is an increasing function going from 0 at p=0 to Rma_X at p=pF. It is shown in Ref. [4] that this procedure amounts to requiring that the nucleons with momentum contained in the interval [p, p+dp] are contributing to the density profile by a horizontal slab corresponding to the vertical coordinates $R(p)$ and $R(p+dp)$, as shown in Fig. 2, or equivalently that nucleons with momentum p do not propagate farther than $R(p)$. The procedure is also equivalent to a phase space joint distribution function of the form

$$\frac{dn}{d^3\vec{r}\,d^3\vec{p}} \propto \frac{\theta(R(p)-r)\theta(p_F-p)}{R(p)^3} \tag{3}$$

where $\theta(x)$ is the Heaviside function. Although this distribution obviously generates correlations between r and p coordinates, it nevertheless yields the constant Fermi gas distribution and the r-space distribution $f(r)$ after integration over $\vec{r}$ and $\vec{p}$, respectively, as demonstrated in Ref. [4]. There are no other correlations. There is no attempt to have zero total momentum ($\sum \vec{p} = 0$), location of the barycenter at the origin ($\sum \vec{r} = 0$) nor zero total angular momentum ($\sum \vec{r} \times \vec{p} = 0$).

All target particles are sitting in a (fixed and constant) attractive square potential well, with a momentum-dependent radius $R(p)$ and a depth $V0$. The function $R(p)$ is such that, in absence of collisions, nucleons are moving while the average (over events) spatial and momentum distributions remain unaffected. This is demonstrated in Ref. [4]. But it is almost clear from Fig.2 that nucleons can be divided into groups of particles with the same momentum

occupying given spheres in *r*-space. In absence of collisions, the distribution in *r*- and *p*-space remains the same on the average (this is a well-known property of a system of billiard board particles with initial momentum and directions at random bouncing elastically on the interior surface of a sphere). We anticipatively indicate that particles with momentum larger than *pF* experience a potential well with radius R_{max} (as for $p = pF$).

The *r-p* correlations introduced in this model are not of the conventional type. They comply with the fact that high (kinetic) energy particles can propagate farther out than low energy particles, as they should, in accordance with the standard shell-model. In contrast with the latter, particles keep the same momentum, be they in the centre or in the (allowed) surface region of the nucleus. The procedure that is adopted here has the advantage of straight-line motion between collisions, an advantage that will become clearer when we will be discussing the propagation of the particles.

B. Projectile preparation

The nucleon is incoming along the *z*-direction and is given at random in the *xy*-plane an impact parameter *b* inside a circle of radius $R_{max} = R_0 + 8a$. A sphere of the same radius centered on the middle of the target is defined as the "volume of calculation". Nothing happens to the particles outside this volume. At t=0 (beginning of the calculation), the incoming nucleon is positioned at the surface of the volume of calculation. As described above, this is also the surface of the potential well felt by this particle. It is considered that at t=0, the incident nucleon has just entered the well. Therefore its total energy has increased by the value of the potential depth *V0* and its momentum has been increased accordingly (direction is not changed; no reflection, no refraction in the entrance channel). The choice of *bmax* guarantees a good compromise between computational efficiency and accurate evaluation of the total reaction cross section. Indeed only a small fraction (10-4) of the interacting events beyond *bmax* is missed.

For an incident pion, the procedure is the same, except that the pion does not experience any average potential. For an incident light ion, the procedure is more involved. First the incident ion has to be generated. In the rest frame of the latter, nucleons are given positions and momenta at random according to Gaussian laws, with rms values given in Table 1 below.

TABLE I. PARAMETERS OF THE GAUSSIAN FORMS USED TO DESCRIBE RADIAL DISTANCE AND MOMENTUM DISTRIBUTIONS IN LIGHT IONS

Light ion	*d*	*t*	^{3}*He*	^{4}*He*
$\sqrt{\langle r^2 \rangle}$ (fm)	1.91	1.8	1.8	1.63
$\sqrt{\langle p^2 \rangle}$ (MeV/c)	77	110	110	153

The values of the parameters are either taken from the Paris potential for the deuteron, and from experiment or from realistic wave functions, for the other ions. In this case, $\sum \vec{r} = 0$ and

$\sum \vec{p} = 0$ are imposed, simply by choosing the values for the last nucleon appropriately, possibly after a renewed generation of the first ones. The maximum impact parameter is taken as *bmax* defined above plus the rms radius of the ion. The transverse position of the ion centre of mass is taken randomly in a circle of radius equal to this new value. The ion is then Lorentz-contracted along the collision axis and the longitudinal position of the ion is chosen in such a way that one of the nucleons is just touching the "interaction volume", the other ones being outside. The ion is then "boosted": 4-momenta undergo the Lorentz transformation corresponding to the velocity of the incident ion. They are finally corrected in order to comply with the energy content of the incoming ion. Because of the generation of the internal motion of the nucleons, the total energy is larger than the nominal incident energy *Winc=Tlab+Minc*. Let us denote by $\varepsilon\imath$ and $\vec{p}_i$ the total energy and the momentum of the ion nucleons, respectively. The momenta of the nucleons are scaled by a common factor such that the sum $\sum \varepsilon\imath$ is put equal to *Winc* . Let us notice that for very slow ions, this operation may not be possible, because the minimum value of $\sum \varepsilon\imath$ is *AincMN*, the mass number of the incident ion times the nucleon mass, whereas the minimum value of *Winc* is equal to that quantity minus the binding energy of the ion. To circumvent this drawback, the following procedure if adopted: if *Winc – AincMN* < 0, all nucleons are given the same kinematics as the velocity as the incident ion, neglecting so internal motion and binding energy. Finally, as in the nuclear case, the nucleon located at the surface of the interaction volume is supposed to sit inside the nuclear potential, with appropriate energy and momentum.

C. Propagation of the particles

At t=0, all nucleons are set in motion with their initial velocity and are assumed to follow straight-line trajectories until an avatar occurs, i.e. until two of them achieve their minimum distance of approach, or until one of them hits the nuclear surface, or until a Δ–resonance decays. Due to the straight-line trajectories, the times at which these events occur can be predicted. The smallest of these times is selected and the particles are propagated in a single step. The simplicity of this propagation is a particular feature of the Liège INC model. After the occurrence of an avatar, straight-line motion is resumed until the next avatar, and so on. The process is followed up and terminated according to a criterion explained below.

Let us elaborate a little bit on the procedure. At the beginning, a table of times for the possible avatars is constructed. For a possible collision between a pair of nucleons *a* and *b*, with initial relative position $\vec{r}_{ab}^{\,0}$ and relative velocity $\vec{\beta}_{ab} = \vec{\beta}_a - \vec{\beta}_b$, the time at which. the relative distance is minimum is given by

$$t_{ab} = -\frac{\vec{r}_{ab}^{\,0} \cdot \vec{\beta}_{ab}}{\beta_{ab}^2} \tag{4}$$

and the square of this minimum relative distance is equal to

$$d_{\min}^2 = \left(\vec{r}_{ab}^{\,\min}\right)^2 = \left(\vec{r}_{ab}^{\,0}\right)^2 - \frac{\left(\vec{r}_{ab}^{\,0} \cdot \vec{\beta}_{ab}\right)^2}{\beta_{ab}^2}, \tag{5}$$

where $\vec{r}_{ab}^{\,\min}$ is the minimum relative position vector. It is also easy to verify that a nucleon *a* will encounter the radius *R* of the potential well (which depends on its momentum) at time

$$t_a = \frac{1}{\beta_a^2}\left[-\vec{r}_a^{\,0}\cdot\vec{\beta}_a + \sqrt{\left(\vec{r}_a^{\,0}\cdot\vec{\beta}_a\right)^2 + \left(R - r_a\right)^2\beta_a^2}\right] \tag{6}$$

See later for Δ-decay. Not all times need to be considered. They are disregarded:

- if they are larger than the stopping time *tstop* of the cascade (see Section 2.F)

- if nucleons *a* and *b* are spectators; nucleons are divided into participants and spectators; a nucleon is a participant if it is an incident nucleon or if it has participated to an avatar (Deltas and pions are participants)

- if *tab* is negative (diverging trajectories)

- if nucleons *a* and *b* are passing too far away from each other to make a real collision, i.e. if $\pi d_{\min}^2 > \sigma_{NN}^{tot}$

- if the c.m. energy of the collision is smaller than 1925 MeV (*2MN+cutNN* , *cutNN* = 48.5 MeV)

The last point needs a word of clarification. Soft collisions are so neglected, for three reasons. First, a soft collision does not change very much the momentum content of the target. Second, most of the time, soft collisions involve nucleons with momenta not far from the Fermi momenta and, therefore, these collisions are expected to be suppressed efficiently by the Pauli principle. The third reason is more practical: taking these soft collisions, whose effect is presumably not important, into account would multiply the number of times *tab*, due to the very large *NN* cross sections at low energy. There are theoretical arguments supporting this procedure, indicating that "soft interactions" are rather taken into account by the average potential, whereas hard interactions contribute to the collisions. See Ref. [16] for a discussion of these matters.

After the list of times for the occurrence of possible avatars is completed, the smallest time of the list is selected. If the corresponding avatar is a collision, a test for the possible realisation of the latter is performed. If

$$\sqrt{s} > 2M_N + cut_{NN} \tag{7}$$

and

$$\pi d_{\min}^2 < \sigma_{NN}^{tot}(s), \tag{8}$$

the avatar is accepted. Otherwise the time *tab* is removed from the list, and the next smallest time is selected. The same test is done and the same procedure is repeated until the avatar is accepted (avatars corresponding to decay or reflection/transmission are always accepted at this stage). Particles are then propagated until the selected time, in a single step.

At this stage, the first avatar is considered for realisation. It may be realized or not (due to Pauli blocking of collisions for instance, see later). If it is realized, the list of times is updated. Let us consider for instance a collision between particles *a* and *b*. We refer here to the labels of the particles. Their nature may have changed during the collisions. All the times involving *a* and *b* are removed. New times are added, corresponding to possible further collisions between either *a* or *b* with other particles (not between *a* and *b* to avoid repeated interactions)

or to possible reflection/transmission of a and b). For other kinds of avatars, it is easy to list the operations needed to update the list of times. Of course, in the addition of new times, the same criteria of selection as described above are applied.

Then, the smallest time of the updated list is selected and the same set of operations is performed, and so on.

The process is terminated on a manner described later.

D. Description of the avatars

D.1 Collisions

Inelastic nucleon-nucleon collisions are dominated by the production of pions. In the energy range mentioned in the introduction, there are good indications that pion production results from the production of a Δ-resonance followed by its decay. Although the Δ-resonance is short-lived, it has a good chance to interact with another nucleon before decaying. The philosophy of the standard INCL model is to propagate the Δ-isobars (instead of describing the NN inelastic collisions by the asymptotic channels in free space). Therefore, the following possible reactions are considered

$$NN \to NN, \quad NN \to N\Delta, \quad N\Delta \to N\Delta, \quad \Delta\Delta \to \Delta\Delta, \quad \pi N \to \Delta \tag{9}$$

We treat the two-body reactions first.

(a) Selection of the final channel. For any of the incident channels (NN, $N\Delta$, $\Delta\Delta$), the final channel is selected at random, by the standard method of comparing a random number with the ratio between elastic and inelastic cross sections. The relevant cross sections, as parametrized in INCL4.2, as well as the angular distributions, are given in Refs. [4,17]. Elastic NN cross sections are of course taken directly from experiment. The $NN \to N\Delta$ cross section is taken as equal to the experimental inelastic NN cross section (pp and np, the nn cross section is taken equal to the pp cross section). The $N\Delta \to NN$ cross section is taken from the previous one by detailed balance:

$$\sigma_{N\Delta\to NN}(s) = f_{corr}\frac{1}{2}\left(\frac{p_{NN}}{p_{N\Delta}}\right)^2 \frac{1}{1+\delta_{NN}}\sigma_{NN\to N\Delta}(s). \tag{10}$$

In this equation, valid for definite charge states of the particles, pab is the momentum of the particles in the c.m.

$$p_{ab} = p_{ab}(s) = \frac{\left[\left(s-(m_a+m_b)^2\right)\left(s-(m_a-m_b)^2\right)\right]^{1/2}}{2\sqrt{s}}, \tag{11}$$

the ½ factor comes from the spin degeneracies and the Kronecker symbol applies to the isospin states of the nucleons. In INCL4, a definite value of the mass is ascribed to the Δ-isobar (see below), which makes $pN\Delta$ well defined. However, detailed balance breaks down for unstable particles. Arguments are given in Ref. [4], which show that the effect of the unstable isobar can be approximated by the use of a correction factor $f_{corr} = \exp(t_{coll}/\tau_\Delta)$ involving the collision time and the Δ lifetime. The former is not well known, but is of the order of 1-2 fm/c. More or less accordingly, in INCL4.2, $fcorr$ is put equal to 3.

The $N\Delta \to N\Delta$ and $\Delta\Delta \to \Delta\Delta$ cross sections are taken as equal to the NN elastic cross section at the same cm energy.

(b) Generation of the final state. The collision is realized in the cm frame. The 4-momenta of the initial particles are Lorentz-transformed in the cm frame. The cm relative momentum q in the final state is calculated by Eq. (11) for the two outgoing particles. For Δ-creating reactions, the mass of the isobar should be determined first. It is taken at random according to the following distribution

$$f(m_\Delta) = F_N \frac{q^3}{q^3 + q_0^3} \frac{1}{1 + 4\left(\frac{m_\Delta - m_\Delta^0}{\Gamma_0}\right)^2}, \tag{12}$$

subject to kinematical constraints: the Δ-mass should be larger than $mN + m\pi$ and smaller than $\sqrt{s} - mN$ (otherwise the available energy is not sufficient). If these conditions are not fulfilled, new random generations are performed repeatedly, until they are satisfied. In Eq. (12), F_N is a normalization constant, q_0=180 MeV/c, m_Δ^0= 1215 MeV and Γ_0=130 MeV. The introduction of the q-dependent factor can be justified as follows: a Δ resonance can be viewed as a πN correlated system and the phase space of the latter is considerably reduced when the cm energy is low. The form of q-dependent factor is also inspired from the πN elastic cross section.

The direction of the outgoing particles (in the cm) are determined according to the experimental angular distributions, as far as possible. The polar angle, relative to the incident direction is taken at random according to distributions which parametrize cm differential cross sections (see Refs. [15,17]). The azimuthal angle is determined at random. The 4-momenta of the outgoing particles are Lorentz-transformed back in the target frame.

For the $NN \to N\Delta$ reaction, the description of the final state is completed with the determination of the Δ-lifetime and of its helicity. The intrinsic lifetime *t0* is determined stochastically according to an exponential law with a mean of $\tau_\Delta = \hbar/\Gamma_0$. The actual lifetime t_Δ is corrected as

$$\frac{1}{t_\Delta} = \frac{1}{\gamma} \frac{q^3}{q^3 + q_0^3} \frac{1}{t_0} \tag{13}$$

where the first factor is the inverse of the Lorentz factor for the motion of the isobar in the target frame and where q is the relative momentum of the pion and the nucleon in the rest frame of the isobar (given by Eq. (11)). The second factor is motivated by the reduction of phase space. The helicity $h = \vec{p} \cdot \vec{s} / |\vec{p}| \cdot |\vec{s}|$ (involving momentum and spin), considered as a classical quantity, is taken at random with a distribution proportional to $\cos^2\theta$, where θ is the angle between the incident direction and the one of the outgoing isobar. The helicity, which is not supposed to change in further (elastic) collisions, will govern the eventual decay of the isobar.

Let us turn to the treatment of the $\pi N \to \Delta$ reaction. The cross section is taken as the experimental πN total cross section and parametrized as follows. The $\pi + p$ cross section is given (in mb) by

$$\sigma_{\pi^+ p} = \frac{326.5}{1+4\left(\frac{\sqrt{s}-1215}{110}\right)^2}\frac{q^3}{q^3+180^3}, \qquad (14)$$

where q (in MeV/c) is the cm relative momentum, given by Eq. (11), and where the cm energy is in MeV. The other πN cross sections are derived by isospin symmetry. Here the generation of the final state is very simple. It consists in creating an isobar with a 4-momentum equal to the sum of the 4-momenta of the pion and the nucleon. Its 3rd component of the isospin is also the sum of the ones of the two incident particles. Finally, its lifetime is generated in exactly the same way as described above and its helicity is taken equal to 1. In INCL4, the $\pi N \to \Delta$ reaction is allowed if the cm energy is larger than 1117 MeV (slightly above the physical threshold) and is smaller than 3 GeV. It is supposed to be elastic only. Above 1500 MeV, the intrinsic average lifetime is taken $\hbar/200\,\mathrm{MeV}$.

D. 2 Reflection/Transmission

At the time foreseen for this kind of avatar, the particle (nucleon or Delta) is sitting on the boarder of its potential well (whose radius depends upon its energy). If its kinetic + potential energy is negative, the particle is reflected. If it is positive, the particle will be transmitted with a probability equal to

$$T = \frac{4kk'}{(k+k')^2}e^{-2G}, \qquad (15)$$

with

$$G = \frac{mzZ_N e^2}{\hbar^2 k'}\left(ar\cos x - x\sqrt{1-x^2}\right), \quad x = \frac{T'}{B}, \qquad B = \frac{zZ_N e^2}{R_0}, \qquad (16)$$

if $x<1$ (below the barrier B) , and $G=0$, if $x>1$ (above the barrier B). In these equations, k and k' are the momenta of the particle before and after transmission, m and z are the mass and charge of the particle, Z_N is the current charge of the target (at the time of the avatar), T' is the asymptotic kinetic energy after transmission and R_0 is the radius of the density distribution. The transmission probability (Eq. (15)) is taken as the product of the transmission of a Schrödinger (plane) wave on a potential step and of the semi-classical (JWKB) transmission probability through a Coulomb barrier $V(r) = B\,R_0/r$, for $r > R_0$, $V(r) = 0$ for $r < R_0$.

When the particle is transmitted, it keeps its direction of motion (there is no refraction). The kinetic energy is changed as $T' = T - V_0$, and the momentum is changed accordingly. Once it is transmitted, the particle is "frozen": it leaves the "interaction volume". Actually, it receives a tag which tells that it should not be considered for further interaction: it will not be accepted any more for the evaluation of the times for future avatars. That is why it receives its asymptotic kinetic energy T' readily. If the particle does not succeed the test for transmission, it is reflected. The times corresponding to this particle are removed from the list of times and new ones (for future avatars involving this particle) are added. See Ref. 5 for a discussion about reflection and refraction.

When the incident particle is a light ion, one can find a slightly different type of avatar, corresponding to the entrance of a nucleon in the "interaction volume". It is reminded that at t=0, only one nucleon is at the boarder of this volume, the other ones being outside. For the latter ones, the time for the entrance is calculated by Eq. (10), where the plus sign is replaced by a minus sign. Reflection is not considered for this kind of avatar. When entering the "interaction volume", the kinetic energy of the nucleon is changed by adding the depth of the potential. The direction is not changed and the momentum is modified accordingly. After the entrance, the list of times is re-actualized in exactly the same way as for the escape of a particle.

D.3 Decay of a Δ particle

At the end of its foreseen lifetime, a Δ-isobar is forced to decay. The decay is performed in the rest frame of the isobar: the pion and the nucleon have opposite momenta (absolute value given by Eq. (11) with $\sqrt{s} = m_\Delta$) and the direction is taken at random with the probability law $P(\theta) \propto 1 + 3h\cos^2\theta$, where θ is the angle between the direction of the isobar (in the lab frame) and the direction of the outgoing pion (the azimuthal angle is chosen completely at random). The 4-momenta of the outgoing particles are Lorentz-transformed back in the target frame. The charge states of the pion and the nucleon are determined in agreement with the isospin Clebsch-Gordan coefficients. The list of the times is updated as described before.

E. Pauli blocking

Due to the fermionic nature of the particles, the collision probability may be diminished as a consequence of the Pauli principle. Although it is a purely quantum effect, the reduction may fortunately be expressed in terms of phase space density. In INCL4, Pauli blocking is implemented in this spirit.

Let us discuss first the case of two body collisions $a + b \to c + d$ with two nucleons in the final state and let $\vec{r}_i$ and $\vec{p}_i$, $i = c, d$, the positions and momenta of the nucleons just after the realization of the collision (the avatar). Phase space occupation probabilities *fi* are estimated by counting the nucleons lying in phase space in a small test volume centered of the representative point of nucleon *i* in phase space. They are given by:

$$f_i = \frac{1}{2} \frac{(2\pi\hbar)^3}{\frac{4\pi}{3} r_{PB}^3 \frac{4\pi}{3} p_{PB}^3} \sum_{k \neq i} \theta\left(r_{PB} - |\vec{r}_k - \vec{r}_i|\right) \theta\left(p_{PB} - |\vec{p}_k - \vec{p}_i|\right), \qquad (17)$$

where the summation runs over nucleons of the same isospin state as nucleon *i* and where θ is the Heaviside function. The factor ½ stands for spin degeneracy (nucleon spin is not considered). The parameters r_{PB} and p_{PB} define the size of the test volume (an hypersphere) in phase space. They should not be too small, otherwise the estimated occupation probability can be vanishing almost all the time and they should not be too large, otherwise the variations of the occupation probability in the occupied phase space can be missed. In INCL4, r_{PB} and p_{PB} have been taken just large enough for results (in typical cases) to be more or less insensitive to moderate modifications on these parameters: r_{PB} =3.18 fm and p_{PB} = 200 MeV/c, which corresponds to ~2.3 natural units of phase space. We remind that in the ground state of normal nuclear matter there is one nucleon (of given spin and isospin) per natural unit. It is generally considered that there cannot be more than one particle per unit phase space in

any circumstance and that this density is more or less achieved in the ground state of actual (at least heavy) nuclei.

The collision will be allowed stochastically with a probability $P=(1-f_c)(1-f_d)$. Pauli blocking is not applied to Δ-isobars (for a collision with a Δ and a nucleon in the final state, there is only one blocking factor). On the other hand, it is enforced for nucleons issued from Δ-decays.

The interplay between this stochastic implementation of the Pauli blocking, the evaluation of the phase space density by Eq. (17) and the fluctuations of the phase space occupancy, inherent to any model with a stochastic generation of the initial state, may introduce unphysical effects, unless sufficient care is exercised. In any particular event, the initial phase space is not uniformly populated and displays "clumps" and "holes". If several nucleons are clumped in a test volume, the quantity f_i may be larger than 1. In such a case, it is put equal to unity. Let us consider the possible effect of a hole in the momentum Fermi sphere. With the procedure described above, the first collision may bring a nucleon into this hole from a higher energy occupied state, creating so a *negative* excitation energy. In order to avoid such an annoying feature, a procedure referred to in Ref. [4] as CDPP (for Consistent Dynamical Pauli Principle) has been implemented. The latter centers on the energy content of the current Fermi sphere. As shown in Section 2.3, the excitation energy of the target may be written as a sum of two terms: one which corresponds to the nucleons which have been promoted above the Fermi level (and which therefore is positive) and a term *ECDPP* which corresponds to the rearrangement of the remaining Fermi sphere and can be considered as the excitation of this remaining Fermi sphere. At each possible collision, after the test on the Fermi blocking is passed successfully, the quantity *ECDPP* is checked for the possible final state. The collision is blocked if *ECDPP* is negative (this check is also done after a Δ-decay, but not after a reflection/transmission, the energy content of the Fermi sphere being not changed in that case). Doing so, the remaining Fermi sphere can only have positive excitation energy. A fortiori, the remaining target (i.e. the baryons inside the "interaction volume") can only have positive excitation energy, in spite of the deficiencies of the implementation of the "statistical" Pauli blocking.

F. End of the cascade

An original feature of INCL4 is the consistent determination of the stopping time, i.e. the time at which the cascade should be stopped. A criterion has been adopted which is based on physical results concerning the time-dependence of several key physical quantities when averaged over events. Examples are given in Fig. 3 below.

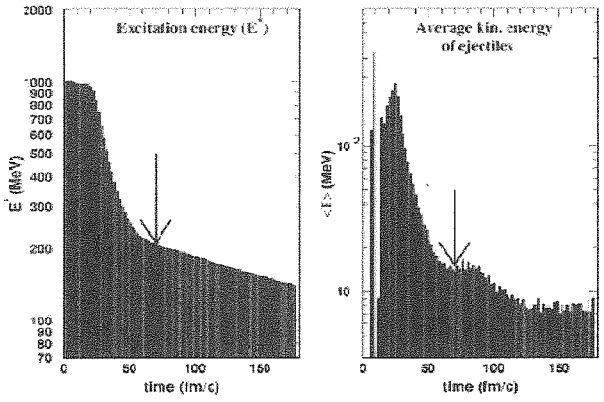

Fig. 3 Time evolution of the excitation of the target nucleus (left) and of the average kinetic energy of the ejectiles (right), as given by averaging over a few thousand events. The results correspond to collisions of 1 GeV protons with 208Pb nuclei at an impact parameter of 4 fm.

One can see that both the excitation energy of the target nucleus and the average kinetic energy of the ejectiles assume large values at early times, decrease rapidly until some time, after which they vary much more slowly. Other quantities (not shown), in particular the anisotropy of the momentum distribution of the participants sitting inside the target, offer a similar pattern with a rapid variation followed by a much slower one. For all of them, the change of regime occurs *at the same time*, defined within a few fm/c. This observation suggests that the regime of fast variation, typical of a cascade, gives place at a rather well-defined time to a regime of softer variation, typical of an evaporation. This feature is also in strong support of skipping an pre-equilibrium module between cascade (at least INCL4.2 with its proper stopping time) and evaporation. We refer to Refs. [4,15,18] for elaboration on this point. In INCL4, the cascade is stopped at this common time, called the stopping time t_{stop}. It has been sampled once for all and parametrized as

$$t_{stop} = f_{stop} t_c \left(\frac{A_T}{208} \right)^{0.16} \tag{18}$$

with f_{stop} =1 and t_c =70 fm/c. This parametric form seems reasonable for the range of energy and target mass under interest, but may be improved at the border of this range, by using another value for f_{stop}. All the results labelled as "INCL4.2" correspond to the standard value of this parameter.

An event is stopped when the clock for a foreseen avatar gives a time larger than t_{stop}. Some events may be stopped earlier. An event may be stopped at the very beginning, if the initial time list for the collision avatars is empty. This happens mainly for peripheral events. Such a event is named a *void event*. An event may also terminate at a time earlier than t_{stop} if the list of times becomes empty when it is updated. In a no-void event, it may happen that no collision has taken place (due to Pauli blocking for instance) and that the incident particle has left the interaction volume with its incident energy. Such events, together with the void events are named "transparent event". The other events are called "interacting events".

Transparent events are just disregarded (but they are counted for cross section evaluation, see later). The other events, after they are stopped, may possibly be completed by the decay of the

remaining Δ-isobars, if any. The Pauli blocking is not applied in this case and the resulting nucleons are considered as belonging to the remnant.

The description of the final state is delayed to Section 2.4

2.3. Conservation laws

It is instructive to detail how INCL4 handles conservation laws. In the energy range of interest, the most important conservation laws can in general be formulated as follows:

$$A_P + A_T = A_{ej} + A_{rem} \tag{19}$$

$$Z_P + Z_T = Z_{ej} + Z_\pi + Z_{rem} \tag{20}$$

$$\vec{p}_P + \vec{p}_T = \vec{p}_{ej} + \vec{p}_\pi + \vec{p}_{rem} \tag{21}$$

$$T_P = K_{ej} + W_\pi + T_{rec} + E^* + S \tag{22}$$

$$\vec{l}_P = \vec{l}_{ej} + \vec{l}_{rem} + \vec{l}^* \tag{23}$$

for baryon number, charge, momentum, energy and angular momentum, respectively. We consider a projectile P colliding with a target T and generating baryonic ejectiles, pions and a remnant (the remaining nucleus at the end of the cascade). For the sake of simplicity, we have assumed that the interaction between the several bodies at the end of the cascade is negligible. In addition, we have disregarded intrinsic spins and we have neglected the production of other particles than those introduced in INCL4. In Eq. (22), K_{ej} is the kinetic energy of the ejectiles, W_π is the total energy of the pions, T_{rec} is the recoil energy of the remnant, $E^*$is the excitation energy of the remnant and S is the separation energy (i.e. minus the Q-value of the reaction). Strictly speaking, energy conservation law should include rest mass energies. They have been eliminated from Eq. (22) owing to the use of Eq. (19). The other notations are self-explanatory.

In INCL4.2, conservation laws (19) and (20) are exactly fulfilled. Eq. (20) is strictly equivalent to the conservation law for the 3rd component of the isospin. Eqs. (21,22) need be commented. Let us for the moment neglect the recoil energy. The different terms of the rhs of Eq. (22) have a well-defined meaning within the INCL4.2 model, in terms of the quantities handled by this model. In addition, since there is no interaction energy in INCL4.2 between the ejectiles, the baryons inside the interaction volume and the pions, decomposition (22) holds at any moment during the cascade. Indeed, one can write, for any time during the cascade

$$T_P + \sum_{i\in A_T}\left(T_i^0 - V_0\right) = \sum_{j}^{A_{ej}} \overline{T}_j + W_\pi + \sum_{i\in A_{rem}}\left(\overline{T}_i - V_0\right), \tag{24}$$

where the sums run over the target nucleons in the initial state, the ejectiles and the baryons remaining in the interaction volume, respectively, and where the bar means that the Δ-nucleon mass difference has been added to the kinetic energy for the isobars (which are supposedly not present any more at the end of the cascade, when Eq. (22) applies). The

quantities T_i^0 are the initial kinetic energies of the target nucleons. In INCL4.2, the interaction volume is fixed and there is no recoil energy. Eq. (24) can be rewritten as

$$T_P = \sum_k^{A_{ej}} \overline{T_k} + W_\pi + \left\{ \sum_{j \in A_{rem}} \overline{T}_j - \left[\sum_{i \in A_T} T_i^0 - (A_T - A_{rem}) T_F \right] \right\} + (A_T - A_{rem})(V_0 - T_F), \qquad (25)$$

where TF is the Fermi kinetic energy. The last term is the minimum energy required to extract $AT - Arem$ nucleons and can be identified as the separation energy S (in the model). Consequently, the term inside the curly bracket is nothing but the excitation energy E* (in the model). This term can still be rewritten as

$$E^* = \sum_{j \in A_{rem}, p_j > p_F} (\overline{T}_i - T_F) + \left\{ \left(\sum_{j \in A_{\min}, p_j \le p_F} \overline{T}_i \right) - \left[\sum_{i \in A_T} T_i^0 - (A_T - A_{rem}^F) T_F \right] \right\}, \qquad (26)$$

where A_{rem}^F is the number of nucleons in the remnant with momentum less than the Fermi momentum. The quantity in the square bracket is the ground state energy of the current Fermi sea. The term in the curly bracket is identified as the excitation energy of the current Fermi sea, i.e. the quantity $ECDPP$ discussed above.

In the INCL4.2 model, energy is conserved exactly, since it is conserved during the collisions and at the entrance and the exit of the interaction volume (but without recoil energy). On the contrary, momentum and angular momentum is not conserved. Momentum is conserved during collisions but not at the entrance or exit of particles. Angular momentum is not conserved, even at the level of the collisions. See however Ref. [3] for a discussion of this topic. However, the results of the cascade can be used to evaluate with reasonable accuracy the momentum, angular momentum and recoil energy of the remnant. The lack of momentum conservation mainly arises from the treatment of transmission of particles at the surface. Suddenly, a particle is emitted with (sometimes a large) momentum $\vec{p}$, without any counterpart. It is not easy to know how to correct for this since it may depend very much upon the dynamics leading to the emission. The simplest thing would be to give an opposite recoil momentum to the nucleus, keeping the same available energy. The momentum of the ejectile relative to the nucleus will then be $\simeq (1 - 1/(2A_{rem}))\vec{p}$. Recoiling the whole remnant (plus the average potential) is technically difficult. But, one can see that the momentum of the ejectiles is estimated in the model with an error of the order of 1/(2A). Therefore, the quantity

$$\tilde{\vec{p}}_{rem} = \vec{p}_p - \vec{p}_{ej} - \vec{p}_\pi \qquad (27)$$

evaluated with the results of the model yields the remnant momentum with an accuracy of the order of 1/(2A). The corresponding recoil energy

$$\tilde{T}_{rem} = \sqrt{\tilde{\vec{p}}_{rem}^2 + M_{rem}^2} - M_{rem} \qquad (28)$$

gives already a good evaluation of the recoil energy of the remnant. It should be stressed that even if $\tilde{\vec{p}}$ can be large part of $\vec{p}_p$, $\tilde{T}_{rem}$ (of the order of 1 MeV) is always very small compared to the other terms of Eq. (22). Nevertheless, in INCL4.2, an effort has been done to include the approximate recoil energy, still managing the energy balance. The recoil energy is first evaluated through Eqs. (27,28). This quantity is then included in the rhs of Eq. (26) and the

momenta of the ejectiles and the pions are multiplied by a factor *f0* in order to balance the two sides of the equation. The modified momenta are then used to re-evaluate $\widetilde{\vec{p}}_{rem}$ and $\widetilde{T}_{rem}$ through Eqs. (27,28). The new recoil energy is introduced in the final energy and the momenta of the ejectiles and pions are multiplied by *f1* in order to balance the two sides of Eq. (26) again, and so on. Two iterations are performed, which is largely sufficient.

The internal angular momentum of the remnant is also evaluated by difference:

$$\widetilde{\vec{l}}^{\,*} = \vec{l}_P - \vec{l}_{ej} - \vec{l}_\pi - \vec{l}_{rem} \tag{29}$$

where the last term is evaluated as $\vec{l}_{rem} = \vec{R}_{rem} \times \widetilde{\vec{p}}_{rem}$, $\vec{R}_{rem}$ being the position of the barycenter of the remnant. It is argued in Ref. [4] that Eq. (29) provides a good estimate, which follows to some extent from the accuracy of the calculated momentum transfer.

2.4. Description of the final state

The output data of a cascade event contain:

1. the type of event: transparent event, absorption (no outgoing particle), non-transparent event (with the number of emitted particles)
2. for each of the emitted particles, the following quantities are recorded:
    1. type of emitted particle
    2. kinetic energy (in MeV)
    3. the three direction cosines
    4. for the remnant: mass number, charge, excitation energy, recoil energy, direction cosines and intrinsic angular momentum (in units of ħ; absolute value and direction cosines).

When coupled to an evaporation model, the output of a (complete) event contains in addition the same information for the evaporated particles and the properties of the final residue. These information are recorded in an *n-tuple*. *n-tuples* can be handled "off-line" by PAW++ to generate physical results.

Evaluation of cross sections is done by standard means. The total inelastic (reaction) cross section is given by:

$$\sigma_R = \pi b_{\max}^2 \left(1 - N_{transp} / N_{run}\right) \tag{30}$$

where N_{run} is the total number of runs and N_{transp} the number of transparent events. Differential cross sections can be formulated as:

$$\frac{d\sigma}{d\varpi} = \pi b_{\max}^2 \frac{N_{i \in d\varpi}}{N_{run} d\varpi}, \tag{31}$$

where $d\varpi$ is the relevant element of phase space and $N_{i \in d\varpi}$ is the cumulated number of relevant particles belonging to this element.

3. A short account of the INCL4.4 model

Here we turn to the recent developments of the INCL4 model that has been added to INCL4.2 to form the INCL4.4 model, as explained in the introduction. Due to lack of space, we only give a sketchy description of the most important features.

3.1. Isospin and energy-dependent potential for nucleons

The motivation for this development is rooted in the phenomenology of the optical model (and of the shell model), which indicates that the depth of the average nuclear potential depends upon the isospin of the nucleons and decreases more or less linearly when the energy of the nucleon increases until it reaches roughly 200 MeV (kinetic energy). At this value, the potential basically vanishes. Above, it remains very small. Accordingly, an isospin and energy-dependent potential for nucleons has been introduced. Square wells with momentum-dependent radius are still used, as before. Inside this radius, the value of the potential is a function $V(\tau,E)$ of the isospin and the total energy E. One now has:

$$E = T + V(\tau,E) = \frac{\hbar^2 k^2}{2M} + V(\tau,E) \tag{32}$$

Following Refs. [19,20], the following form is used

$$V(\tau,E) = V_0(\tau) + \alpha_\tau \left(E - E_F^\tau\right), \qquad \text{for } E < E_0^\tau,$$

$$V(\tau,E) = 0, \qquad \text{for } E > E_0^\tau, \tag{33}$$

where E_F^τ is the Fermi energy and E_0^τ is the energy at which the rhs in the first line vanishes. For the sake of consistency, the Fermi momentum should also depend upon isospin, in order to have roughly the same Fermi energy for protons and neutrons, which is required by β-stability. The Fermi momenta are determined by

$$\left(\frac{k_F^n}{k_F^p}\right)^3 = \frac{N}{Z}, \quad \frac{1}{3\pi^2}\left[\left(k_F^n\right)^3 + \left(k_F^p\right)^3\right] = \rho_0 \tag{34}$$

translating the fact that neutron and proton densities are proportional to neutron and proton mass numbers and sum to ordinary nuclear density. The parameters α_τ in Eq. (33) are taken as $\alpha_p = \alpha_n = 0.23$, following Ref. [19]. Finally, the quantities $V_0(\tau)$ are determined by requiring

$$E_F^\tau + T_F^\tau + V_0(\tau) = -S_\tau, \tag{35}$$

where S is the separation energy. The potential for Δ-isobars is kept energy-independent but does depend upon the isospin, with a linear dependence which matches the one for protons and neutrons. The potential depth for the Δ-isobars is determined by assuming that, for the same isospin, it is equal to the nucleon potential at the Fermi energy.

The implementation of such a potential somehow complicates the realization of collisions. Indeed, for collisions $a + b \to c + d$, the energy conservation now writes

$$E_a + V_a + E_b + V_b = E_c + V_c + E_d + V_d \qquad (36)$$

in the rest frame of the potential (or the target). It is proceeded as follows. The initial free 4-vectors $(E, \vec{p})$ are Lorentz-transformed into the usual cm frame (as before). The corresponding final 4-vectors in this frame are determined, as usual, i.e. conserving momentum and free (kinetic) energy. This would be the normal procedure if there were no potential. Let p* be the momentum of the particles in the cm. Let us consider now these 4-vectors after multiplication of p* by a factor f* (and, of course, after modification of the energy component to be consistent with the cm energy). These modified 4-vectors are Lorentz-transformed back in the target frame and inserted in Eq. (36), which appears then as an algebraic equation for f*. So the new energy conservation law is fulfilled owing to solution of this algebraic equation. It turns out that f* is always rather close to unity. This may suggest that the energy-dependence of the potential has minor effects. Actually, the effect may be significant when, in a collision, nucleons changes substantially their individual energy. Of course, it is expected that there are compensating effects in other collisions. It is therefore no surprise that the effect of the energy-dependence is noticeable for charge-exchange quasi-elastic and quasi-inelastic events (see ref. [18]).

3.2. Average potential for pions

A difficulty arises here. The phenomenological optical-model potential for pions is badly determined in the nuclear volume, because of the strong pion absorption. Propagating pions are not therefore good quasi-particle excitations. Furthermore, what is needed is the potential energy of a pion created at any moment of the multiple scattering process (involving successive creations and absorptions of pions), which of course cannot be revealed by elastic scattering experiments to which the optical model applies. Finally, the largest part of the pion-nucleon interaction proceeds to Delta formation, which is explicitly accounted for in INCL. In view of these considerations, a pragmatic approach has been adopted. A square well potential is chosen with a radius of $R_c = R_0 +$ 2fm, a range somehow consistent with the properties of the empirical pion potentials. More precisely, the following form is used:

$$V(r,\tau) = V_t(\tau) = V_N(\tau) + \overline{V_C}\,, \qquad \text{for } r < R_c\,, \qquad (37)$$

$$V(r,\tau) = V_C = \frac{Z_T \tau e^2}{r}\,, \qquad \text{for } r > R_c\,,$$

where τ is the 3rd component of the pion isospin. The nuclear part VN and the average Coulomb part $\overline{V_C}$ are given by

$$V_N(\tau) = V_N^0 + V_N^1 \tau\xi\,, \qquad \overline{V_C} = 1.25\frac{Z_T \tau e^2}{R_0} \qquad (38)$$

where $\xi = (N\text{-}Z)/A$ is the asymmetry parameter of the target.

The parameters V_N^0 and V_N^1 have been determined by a rough fit to experimental data concerning reactions with pions as incident or produced particles. The following values have been so obtained: V_N^0 = -30.6 MeV and V_N^1 = -71.0 MeV, rather consistently with the phenomenological values of the pion potential in the nuclear surface.

Pions are now considered as participants. They are subject to transmission or reflection at the boarder of their nuclear potential (using formulae (15,16)) and they do not interact any more after leaving this potential.

The introduction of the pion potential considerably improves the predictions of INCL4 for the pion production cross sections, but also, to a lesser extent, for other observables. See Refs. [11,18] for more detail.

3.3. Production of light charged clusters

The introduction of this production is based on the idea that a nucleon escaping from the nucleus can drag with him other nucleons which are sufficiently close (in phase space), and form an emitted light charged cluster. The following procedure has been introduced:

1. When a nucleon hits the surface and satisfies successfully the test for emission (sufficient energy), it is checked to see whether it can belong to a cluster. A candidate cluster is constructed, starting from the considered nucleon, by adding a second, then a third, etc, nucleons which are sufficiently close in phase space. The following proximity criterion is adopted:

$$r_{i,[i-1]}\, p_{i,[i-1]} \leq h \ , \tag{39}$$

   where the quantities in the lhs are the Jacobian coordinates, i.e. the relative spatial and momentum coordinates of nucleon i with respect to the subgroup consisting of the first i-1 nucleons, and where h is a parameter. The following light clusters are considered for the moment: d, t, ^3He, ^4He. Δ-isobars are not supposed to be included in clusters.

2. Fast nucleons being checked for emission at $R(pF)$, in the very outskirts of the nuclear surface, where the density is practically vanishing, they are moved back along their direction of motion until they sit at a radial distance $R_0 + D$ (One is forced to check for emission of nucleons at large radial distance, because possible collisions even in the periphery of the nucleus cannot be precluded). In order to avoid problems with tangential emission, clusters are considered only if the cosine of the angle between their emission direction and the radial direction is larger than a certain value, taken as 0.7.

3. The cluster with the lowest "excitation energy" is selected. The relevant parameter is $\left(\sqrt{s} - B\right)/A$, where $\sqrt{s}$ is the c.m. energy of the cluster, B its nominal binding energy, and A its mass number.

4. For being emitted, the selected cluster should fulfil two requirements. First, its total kinetic plus potential energy, corrected by the nominal binding energy should be positive, owing to which a cluster with positive kinetic energy can be emitted. Second, it has to succeed the test for penetration through the Coulomb barrier, given by Eqs. (16,17). If these conditions are not met, the "leading" nucleon is emitted, provided it succeeds the Coulomb penetration test.

Let us notice that this procedure is slightly different from the one described in Ref. [9] and used in INCL4.3. In the latter, only one cluster for each species was constructed and a hierarchy for the possible emission was established, favoring emission of heavier clusters. See Ref. [9] for more detail.

The procedure described above looks like a surface coalescence model and retains some well established features: the small probability for existence of clusters in the nuclear volume and the necessary dynamical generation of clusters in the surface from "pre-existing" clusters. It contrasts with the ordinary coalescence model: clusters can be emitted at any time and their properties are not directly linked with the final nucleon spectra. It contains two parameters: D and h. They have tentatively been determined by a rough fit to experiment. The extracted values are D=2fm and h=387 MeV fm/c.

This model cures evidently a serious shortcoming of INC models. Furthermore, it gives surprisingly good results, at least for sufficiently high enough incident kinetic energy. See Ref. [9] for detail. To extend this model at lower energy, variation of the parameters and modification of the scenario are presently envisaged [14].

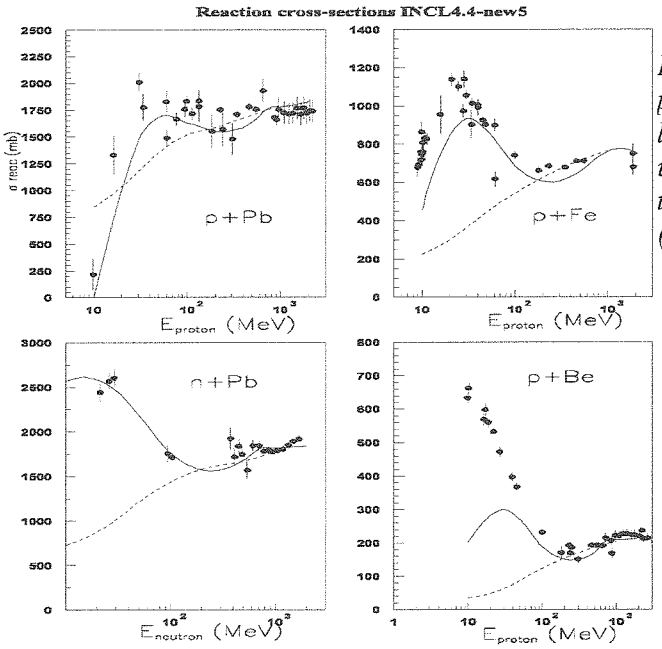

Fig. 4. Comparison of the predictions of INCL4.2 (dashed-lower lines) and of INCL4.4 (full upper lines) with the experimental total reaction cross sections (collected from Refs.[23,24]).

3.4. Extension to low energy

The conventional wisdom expresses that the INC approach is valid in the classical (non quantum) independent collision regime, which roughly requires that the following condition is fulfilled:

$$\lambda\!\!\!^{-}_B << r_s < d\,, \tag{40}$$

where $\lambda\!\!\!^{-}_B$ is the de Broglie wavelength for the relative motion, r_s is the range of the nuclear forces and d is the average distance between neighbouring nucleons. These conditions are only marginally satisfied (and for the first collisions only) for incident energy above 200 MeV. Yet, INC models do not seem to yield crazy results at lower energy. Even, it was shown in Refs. [12,21] that INCL4.2 can reproduce surprisingly well neutron and proton spectra at as low incident energy as 50 MeV, where important quantum motion effects are expected. There is no real explanation to this paradox. See however Ref. [22] for an interesting discussion.

The most important deficiency of INC4.2 at very low energy lies in the fact that it is unable to reproduce the rise of the total cross section just above the Coulomb barrier. The latter is

usually interpreted as due to the interplay between the rise of the *NN* cross section and the variation of the penetration through the Coulomb barrier. Several ways of curing this defect have been investigated recently [14], resulting in a much better prediction of the total reaction cross section, as shown in Fig.4. Because of lack of space and because these developments are still under investigation, we cannot give much detail here. Let us just mention that the quantity cut_{NN} has been removed (set to zero) for the first collision, Coulomb distortion in the entrance channel has been introduced and corrections have been introduced to compensate for the too large momentum content of the target surface (see Section 2.2.A). One may wonder why cut_{NN} has been removed whereas we have insisted on cutting soft collisions. In fact, soft collisions do not perturb very much the nucleon motion and it is then natural (or acceptable) to consider that their effect is mainly taken into account by the average potential. However, the total reaction cross section is determined by the first collision inside any event. Whether the first collision is soft or hard does not matter, inasmuch a soft collision can be followed by a harder one. It is then indicated to consider first soft collisions totally.

The last modification deals with collisions occurring in the nuclear surface. As we said in Section 2.2.A, the target nucleons moving in this region have a large energy (in the allowed [*0, TF*] interval). They have also a large momentum. This results from the use of square well potentials. It is generally considered that, in reality, these nucleons have a large energy but a low momentum, in accordance with the shell-model, which uses a smooth Saxon-Woods-like potential. Let us now consider the collision between an incident low-energy nucleon and one of these surface target nucleons. If the cross section depends upon the relative momentum, the latter is probably overestimated in INCL4.2 and the cross section is consequently underestimated. To compensate for this, a new procedure have been introduced, which realizes the collision with the momenta of the particles in a smooth potential, defined as having the same classical turning points as the one used in INCL4.2. The latter is implicitly given by

$$V(r) = V(r = R(p)) = -V_0 + \frac{\left[p = R^{-1}(r)\right]^2}{2m}, \tag{41}$$

where R^{-1} is the inverse of the function *R(p)*. In practice, the modified momenta are calculated, by using this potential. The collision is realized with this kinematics, including the evaluation of the cross section, and the final momenta and energies are calculated after restauration of the original INCL4.2 potential, guaranteeing so the conservation of energy. It is easy to see that this modification has no effect when the collisions occurs in the interior (the potential defined by Eq. (41) is practically equal to $-V_0$ in this region) or when the collision occurs at high energy. One should also realize that this procedure has to do with the extrapolation of the experimental cross sections to off-shell particles. The original procedure of INCL4.2 supposes that the cross sections should be extended according to the cm energy, whereas the new procedure is better suited if they have to be extended according the momenta of the particles. More details are given in Ref. [15].

One has to stress that, even if the modifications described in this subsection are motivated by the behaviour of INCL4.2 at low incident energy, they have been implemented for any incident energy. It is easy to see that they are only effective at low energy.

3.5. Other modifications

Other minor modifications have also been introduced in the meantime. Let us mention two of them:

1. The strict Pauli blocking has been introduced on the first collision. This seems to be the best compromise which minimizes the problems inherent to the statistical implementation, partly cured by the CDPP procedure (see Section 2.2.E), and accounts nevertheless for the depletion of the Fermi sphere. More detail can be found in Ref. [21].

2. Events are terminated at *tstop* (see Section 2.2.F) or when all the particles have energies below the Fermi energy plus a constant energy, taken as 10 MeV, if this occurs earlier. In such a situation, it is expected that the system will basically evolves by evaporation. This new procedure has been adopted because the results are basically unchanged, while the computation time is reduced by 25%.

4. Outlook

We have presented an analytical description of the recent versions of the INCL model, trying to present the features of the physics included in this model, the various assumptions and some technical points, which are nevertheless important to understand how the numerical simulations are working.

The standard version INCL4.2 is basically a parameter free version. In the numerical code, there are only two physical parameters: the potential depth *V0* and the nucleon separation energy. These are not really free parameters, as it is indicated to use phenomenological values for these parameters. There are also options allowing to use a more or less diffuse surface, to vary the stopping time (through the parameter *fstop*) and to adopt alternative versions of the Pauli blocking (like the strict Pauli blocking), enabling the user to have an idea of variations of the model. But it should be stressed that what is referred to as the INCL4.2 model corresponds to the standard choice described in this paper.

We did not discuss the performances of INCL4.2. For this, we refer to Ref. [4]. One has to keep in mind that if some observables constrain the INCL model alone (total reaction cross section, high-energy particle spectra), many others constrain INCL and the de-excitation model to which it is coupled, at the same time. The good performances of INCL4.2 for the second kind of observables have been obtained thanks to the coupling to the standard version of the ABLA model (named KHSv3p, see Ref.[4]). They have to be confirmed with the new version of ABLA [6] or with another evaporation-fission model.

Model INCL4.4 has been developed to cure some shortcomings of INCL4.2 (lack of cluster emission), to introduce mandatory features of nuclear dynamics (energy-dependent average potential for nucleons and average potential for pions) and to improve the performances, especially at low energy. Inclusion of new features was done by relying as much as possible on known physics rather than on free parameters. Developments are still in progress, but it is likely that achieving a good description of more and more observables in a more and more extended domain will not be possible with a little dose of free parameters. We have particularly in mind the production of clusters, which is expected to proceed differently at high or low incident energy and in heavy or light nuclei. Preliminary results seems to indicate that the goal could be reached with a satisfactorily low level of fitting procedure [14,25].

We did not really discuss the justification of the assumptions of the model, nor the general theoretical foundation of the model, which is still in embryo for the time being. See Ref. [15] for a discussion of this point.

ACKNOWLEDGEMENTS

We want to thank all the people with whom we had the pleasure to collaborate on the developments of the Liège Intranuclear Cascade model since the beginning and, in particular, those who have contributed to INCL4 in the recent years: Thierry Aoust, Pierre Henrotte, Sylvie Leray, Sophie Pedoux, Claude Volant and Yair Yariv.

This work has been done in the frame of the EU IP EUROTRANS project (European Union Contract N° FI6W-CT-2004-516520). We acknowledge the EU financial support.

REFERENCES

[1] J. Cugnon, T. Mizutani and J. Vandermeulen, Nucl. Phys. **A352** (1981) 505
[2] J. Cugnon, Nucl. Phys. **A462** (1987) 1987
[3] J. Cugnon, C. Volant and S. Vuillier, Nucl. Phys. **A620** (1997) 475
[4] A. Boudard, J. Cugnon, S. Leray and C. Volant, Phys. Rev. C**66** (2002) 044615
[5] J.-P. Meulders et al, *HINDAS Detailed Final Report*, EU Report, 2005
[6] K.-H. Schmidt, these proceedings and references therein
[7] R.E. Prael and H. Liechtenstein, report LA-UR-89-3014, Los Alamos National Laboratory, (1989)
[8] J.S. Hendricks et al, ORNL Report ORNL-TM-196 (2003)
[9] A. Boudard, J. Cugnon, S. Leray and C. Volant, Nucl. Phys. **A740** (2004) 195
[10] Th. Aoust and J. Cugnon, Eur. Phys. J. **A21** (2004) 79
[11] Th. Aoust and J. Cugnon, Phys. Rev. C. **74** (2006) 064607
[12] J. Cugnon and P. Henrotte, Eur. Phys. J. **A16** (2003) 393
[13] Th. Aoust, A. Boudard, J. Cugnon, J.-C. David, P. Henrotte, S. Leray and C. Volant, NIM Phys. Res. **A562** (2006) 806
[14] A. Boudard, Proceedings of the *Nice Nuclear Data 2007 Conference*, to be published
[15] J. Cugnon, http://www.theo.phys.ulg.ac.be/~cugnon/
[16] J. Cugnon, Ann. Phys. Fr. **21** (1996) 537
[17] J. Cugnon, D. L'Hôte and J. Vandermeulen, NIM **B111** (1996) 215
[18] Th. Aoust, PhD thesis, University of Liège, 2007
[19] C. Mahaux and R. Sartor, Adv. Nucl. Phys. **20** (1991) 1
[20] P.E. Hodgson, "*The Nucleon Optical Potential*", World Scientific, Singapore, 1994
[21] P. Henrotte, PhD thesis, University of Liège, 2005
[22] Y. Yariv et al, Proceedings of the *Nice Nuclear Data 2007 Conference*, to be published
[23] R.E. Prael and M.B. Chadwick, report LA-UR-97-1744, Los Alamos National Laboratory, (1997)
[24] B.C. Barashenkov, *Cross Sections of Interactions of Particles and Nuclei with Nuclei, JINR Publications*, Dubna, (1993)
[25] Th. Aoust et al, NIM Phys. Res. **A562** (2006) 806